Available online at www.sciencedirect.com

SciVerse ScienceDirect

Scripta Materialia 67 (2012) 439–442

Scripta MATERIALIA

www.elsevier.com/locate/scriptamat

Effect of grain size on prismatic slip in Mg–3Al–1Zn alloy

S.M. Razavi,[a] D.C. Foley,[b] I. Karaman,[a,b,*] K.T. Hartwig,[a,b] O. Duygulu,[c] L.J. Kecskes,[d] S.N. Mathaudhu[d] and V.H. Hammond[d]

[a] *Department of Mechanical Engineering, Texas A&M University, College Station, TX 77843, USA*
[b] *Materials Science and Engineering Graduate Program, Texas A&M University, College Station, TX 77843, USA*
[c] *TUBITAK MRC, Materials Institute, Gebze, Kocaeli 41470, Turkey*
[d] *US Army Research Laboratory, Weapons and Materials Research Directorate, Aberdeen Proving Ground, MD 21005, USA*

Received 21 February 2012; revised 8 May 2012; accepted 15 May 2012
Available online 29 May 2012

The grain size of Mg–3Al–1Zn magnesium alloy was systematically varied from 33 μm down to 350 nm, while keeping the crystallographic texture nearly constant, via multi-temperature equal-channel angular processing. Nearly the same texture allowed the activation of mostly prismatic slip in tension and thus evaluation of the effect of grain size on prismatic slip. The maximum tensile yield strength of 385 MPa and ultimate tensile strength of 455 MPa were achieved in materials with an average grain size of 350 nm, accompanied with 13% ductility.

Keywords: Prismatic slip; Magnesium alloys; Equal-channel angular pressing/extrusion; Grain size; Hall–Petch relation

Magnesium alloys have recently attracted great interest due to their lightweight and high specific strength [1]. However, because of their hexagonal close-packed structure, they have few active slip systems, resulting in poor formability, and high mechanical anisotropy at room temperature. Equal-channel angular processing (ECAP) enhances both the strength and ductility of these alloys by reducing their grain size and altering the crystallographic texture [2–4]. In most studies on Mg alloys involving ECAP, processing was carried out at 200 °C or above, which triggers dynamic recrystallization (DRX) [3,5]. DRX can strengthen the alloys by introducing fine grains down to an average size of a few microns. However, for further strengthening, it is necessary to process these materials at lower temperatures to prevent DRX and refine the microstructure through severe plastic deformation [5–7].

To refine the grain size of Mg alloys below 1 μm, the multi-temperature step-down ECAP approach has been developed [5–8]. The processing by Ding et al. [5] for AZ31 Mg alloy consisted of 12 ECAP passes at various temperatures using a 120° angle die. The lowest processing temperature was 115 °C, and the average grain size was ~370 nm. These materials demonstrated yield and ultimate tensile strengths (UTS) of 372 and 445 MPa, respectively, along the extrusion direction with a tensile ductility of 10%. However, the mechanical response along other directions was not reported. Later, Biswas et al. [6] were able to ECAP pure magnesium at room temperature using this technique and achieve an average grain size of 250 nm. However, the resulting mechanical properties were not reported. Recently, Foley et al. [8] processed AZ31 following a five-step hybrid ECAP route using a 90 degree angle die and decreased the processing temperature from 200 °C in the first pass to 125 °C for the last pass. However, they only presented compression responses with a maximum yield strength of 350 MPa. All of these studies were mainly concerned with grain refinement by reducing processing temperature without a detailed discussion on post-processing room-temperature deformation mechanisms and their relations to grain size and texture.

In Mg alloys, the critical resolved shear stress (CRSS) values for non-basal slip modes are much higher than those for basal slip [9]. Activation of prismatic slip, however, has been seen at room temperature when the loading axis is perpendicular to the basal plane normal

* Corresponding author at: Department of Mechanical Engineering, Texas A&M University, College Station, TX 77843, USA. Tel.: +1 979 862 3923; fax: +1 979 862 2418.; e-mail: ikaraman@tamu.edu

1359-6462/$ - see front matter © 2012 Acta Materialia Inc. Published by Elsevier Ltd. All rights reserved.
http://dx.doi.org/10.1016/j.scriptamat.2012.05.017

[10–14]. Some of the recent works also reported the grain size dependence of prismatic slip, especially in AZ31 alloy [12,14], though only down to grain sizes larger than 1 μm.

In the present work, a systematic ECAP study was performed utilizing a multi-temperature step-down technique to incrementally refine the grain size while keeping the crystallographic texture almost the same. The purpose of the latter was to activate mainly prismatic slip under tension at room temperature without a texture variation to evaluate the grain size dependence of prismatic slip down to submicron scale. Due to the higher initial CRSS of prismatic slip, the grain refinement is expected to be more effective in strengthening of AZ31 for the textures mainly favoring prismatic slip, as compared to those favoring basal slip and twinning. This approach will help evaluate the maximum potential of grain size refinement for strengthening Mg alloys.

A hot-rolled plate AZ31 was cut into square cross-section billets with the dimensions of $25 \times 25 \times 150\ mm^3$. ECAP was conducted in a 90° die with sharp corners at the channel intersection. The necessary ECAP parameters (i.e. extrusion rate, back-pressure level, and sequence of the temperature level and routes) were determined, after many trials, to avoid major shear localization and twinning during processing, and to obtain and maintain the desired crystallographic texture and submicron grain sizes. However, only hybrid routes that succeeded in creating prismatic slip under subsequent tension at room temperature are reported here. More detailed information on the process design can be found in Ref. [15].

The starting material had a strong basal texture aligned with the plate normal. The billets were inserted in the ECAP die at 200 °C with the basal poles parallel to the extrusion direction (ED) for the first pass (Fig. 1). This texture alignment was selected because more DRX occurs during ECAP at 200 °C in AZ31 with this starting condition, which results in more grain refinement in the first pass as compared to other configurations [7].

Three billets were processed with the processing schedules described in Table 1. The first billet was processed following four passes of route A (4A) at 200 °C to develop a refined and homogeneous microstructure. The other two billets were processed in the same way as billet no. 1, but they were given additional ECAP passes. For billet no. 2, the temperature was reduced to 150 °C after 4A at 200 °C, to suppress grain growth. A 180° rotation around ED (route C) was applied prior to the processing at 150 °C (4A + 1C). This route, was selected to suppress twinning during processing, which results in deformation localization and failure [16], and to orient the basal planes favorably along the ECAP shear plane for easy activation of basal slip. This method should increase the basal dislocation density, strain harden the basal slip, and reduce the CRSS ratio of the non-basal to basal slip [6]. Billet no. 3 was processed similarly to billet no. 2 with one more pass at 125 °C following route C (a 180° rotation at the temperature reduction step, 4A + 1C + 1C). The extrusion rate was kept at $0.075\ mm\ s^{-1}$ for all passes except the last one at 125 °C in billet no. 3, which was reduced to $0.038\ mm\ s^{-1}$ to suppress shear localization [8,16]. The actively applied back-pressure was 30 MPa at 200 °C, 50 MPa at 150 °C, and 70 MPa at 125 °C.

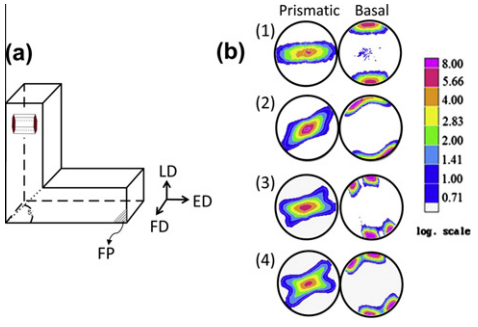

Figure 1. (a) Schematic showing the initial orientation of basal poles in the die prior to the first ECAP passes and the three orthogonal directions. (b) Basal and prismatic pole figures of (1) as-received, (2) 4A, (3) 4A + 1C, (4) 4A + 1C + 1C AZ31 samples. ED, extrusion direction; FD, flow direction; LD, longitudinal direction; FP, flow plane.

Specimens for optical microscopy were cut parallel to the flow plane (FP) from the fully deformed region of the billets. See Figure 1 for the definition of the principal planes of the billet. After mechanical polishing, the specimens were etched in a picral solution and examined using a JEOL 7500F field-emission scanning electron microscope. For transmission electron microscopy (TEM), the specimens were cut from the FP, mechanically ground and ion milled. The foils were examined with a JEOL 2100 microscope.

Tensile samples were cut with the tensile axis along the FD. Tension tests were performed at a strain rate of $5 \times 10^{-4}\ s^{-1}$ using an MTS test frame. The gauge sections of the tensile specimens were $8 \times 3 \times 1.5$ mm. An extensometer with an 8 mm gauge length was directly attached to the samples for strain measurement. Three to five tests were conducted to check the repeatability of the experiments. Texture measurements were carried out on the FP using a Bruker D8 Discover Diffractometer with Cu K_α radiation.

Figure 1b shows the basal and prismatic pole figures for the as-received material and the three ECAP cases. The ECAP textures are similar to each other, having two separate peaks: one approximately along LD and the other almost 45° from LD. In all samples, including the as-received material, the basal poles are almost perpendicular to FD because they are close to the rim of the pole figures. Based on the previous reports, when the c-axis is constrained and extension twinning is not favorable due to texture, prismatic slip should be the main mode of deformation in AZ31 [12,14,17]. Therefore, regardless of the exact locations of the basal poles in the present case, the fact that they are primarily along the rim of the pole figure should ensure the activation of mostly prismatic slip under tension along FD.

The starting material has nearly equiaxed grains with an average size of 33 μm. The microstructures observed in the three ECAP cases are presented in Figure 2. In all cases, a homogeneous microstructure is evident. The average size of 200–300 grains was measured for all cases and their size distributions are depicted in Figure 2d. As listed in Table 1, the grains were significantly refined at each step. In the 4A + 1C + 1C case, grain

Table 1. Processing conditions for the three AZ31 Mg billets examined in this study. The error ranges for the mechanical test results represent the standard deviations from the experiments on three to five companion specimens.

No. of cases	Processing	Symbol	Average grain size (μm)	0.2% proof stress (MPa)	UTS (MPa)	Elongation-to-failure (%)
1	4 passes of route A at 200 °C	4A	2.9 ± 1.3	244 ± 0.5	314 ± 3	12.2 ± 1.2
2	4A plus a 180° rotation, then one additional pass at 150 °C	4A + 1C	0.59 ± 0.20	304 ± 6	372 ± 8	15.7 ± 0.3
3	4A + 1C plus a 180° rotation, followed by a final pass at 125 °C	4A + 1C + 1C	0.35 ± 0.10	385 ± 6	455 ± 4	12.7 ± 1.2

sizes were as low as ~350 nm. For this case, TEM was used to check the validity of the scanning electron microscopy (SEM) observations since the grains were quite small. The grain sizes in the TEM images (Fig. 3) were comparable to those from the SEM images. No twinning was seen in this ultrafine-grained sample.

The room temperature mechanical responses of the ECAP and as-received samples along FD (along the transverse direction the hot-rolled samples) are shown in Figure 4a. There is a significant improvement in the yield strength as the grain size is refined by lowering the processing temperature in subsequent ECAP passes. The 0.2% proof stress increases from 158 MPa in the as-received samples to ~385 MPa in the 4A + 1C + 1C sample. The latter also demonstrated an UTS of 455 MPa with almost 13% tensile ductility. To the best of the authors' knowledge, the yield strength achieved in the 4A + 1C + 1C sample is the highest for AZ31 Mg alloy reported so far, with substantial tensile ductility.

The mechanical properties of all the cases are summarized in Table 1. Since the textures generated for all cases are similar for the purpose of mostly activating prismatic slip, it can be stated that the improvement in strength is mainly because of the grain refinement achieved during ECAP. There are clearly minor differences in the basal pole spread towards FD in Figure 1b; however, this should have only a minor influence on the activation of prismatic slip and macroyield strength. It is possible that the onset of microyielding might involve some basal slip activity; yet, macroplasticity should be governed by prismatic slip. Indeed, similar arguments

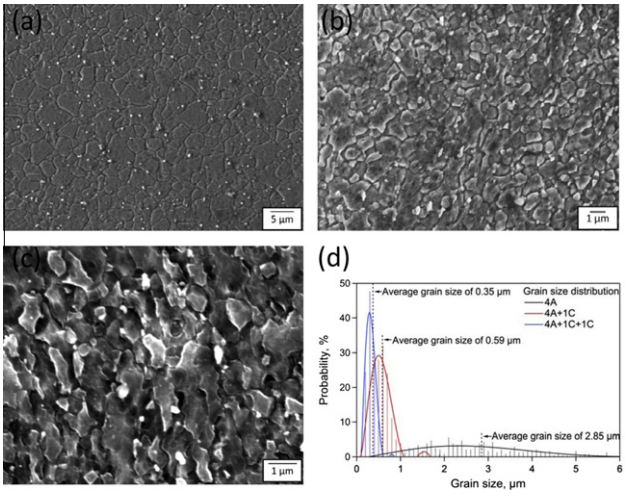

Figure 2. SEM showing fine-grained microstructures of (a) 4A, (b) 4A + 1C, (c) 4A + 1C + 1C ECAP processed AZ31 samples, and (d) corresponding grain size distributions.

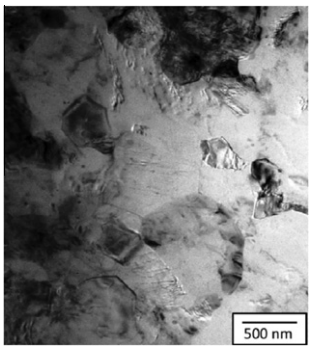

Figure 3. TEM image showing the ultrafine-grained structure of the 4A + 1C + 1C average grain size of 350 nm.

on the activation of prismatic slip for this kind of textures have been made recently [11,12,14] and prismatic slip at room temperature was reported in several earlier studies [18,19].

Since prismatic slip is the main deformation mode and the flow stress increases with decreasing grain size in the experiments shown in Figure 4, it can be inferred that reduction in grain size increases the CRSS for prismatic slip. Figure 4b shows the Hall–Petch (H-P) plot for the 0.2% offset proof stress values in the present work and what have been reported in the literature for prismatic slip in AZ31 Mg alloy. A single best-fit line was drawn for all data points. Using the standard H-P relation:

$$\sigma_y = \sigma_0 + k_y d^{-1/2},$$

where σ_0 is the friction stress against dislocation motion and k_y is the H-P slope; k_y is determined to be 150 MPa $\mu m^{1/2}$ and σ_0 to be 143 MPa (not shown in the figure). Yuan et al. [14] found k_y and σ_0 to be 236 MPa $\mu m^{1/2}$ and 103 MPa, respectively, for the AZ31 samples with average grain sizes between 1.4 and 10.2 μm. However, after combining their results with those for the samples with average grain sizes of 0.7 μm and above [20,21], σ_0 increased to 145 MPa and k_y decreased to 157 MPa $\mu m^{1/2}$. Similarly, if we consider all the data collected from the literature along with the present results for average grain sizes > 2 μm, k_y and σ_0 are measured to be 205 MPa $\mu m^{1/2}$ and 124 MPa, respectively. This and the data points below 2 μm in Figure 4b clearly indicate that with the reduction in grain size below 1–2 μm, the yield strength does not increase as much as expected from the H-P response of the samples with larger grain sizes.

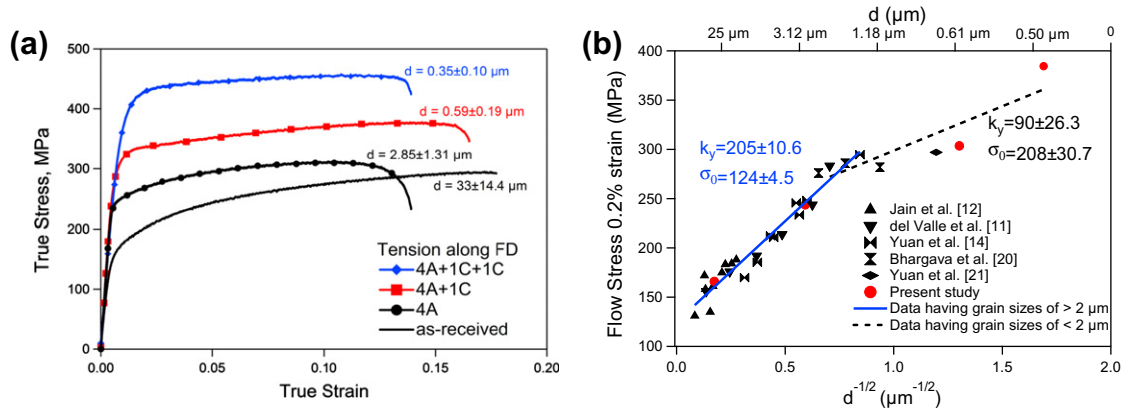

Figure 4. (a) Room temperature true stress vs. strain curves for AZ31 Mg alloy samples with different grain sizes in tension along FD. Prismatic slip should be the main deformation mechanism in the plastic region due to the textures shown in Figure 1. (b) Corresponding Hall–Petch (H-P) plot for prismatic slip including the data from the literature. One plot only includes the data for grain sizes >1 μm, the other plot consists of grain sizes down to 350 nm. k_y is the H-P slope.

One possible reason for the reduction in the H-P slope and yield strength, when submicron grain sizes are considered, is the spread in the basal textures towards FD and the likelihood of the basal slip activation prior to prismatic slip in small grain sizes. It is known that basal slip is notably less grain size dependent than prismatic slip [12], and the reduction in grain size may postpone the activation of prismatic slip in the presence of the basal pole spread. Alternatively, there may be a critical grain size where prismatic slip ceases to be the main yield mechanism in this loading condition. If pyramidal $\langle c + a \rangle$ slip is activated instead, this may indicate a lower grain-size sensitivity for pyramidal slip compared to prismatic slip. The change in the grain boundary character in the samples with submicron grain sizes can also be influential. As the number of ECAP passes increases, the material is further textured while the grain size gets smaller, and the fraction of low-angle grain boundaries should increase, resulting in the observed softening effect in the yield strength. Electron back-scattered diffraction imaging can be used to monitor the grain boundary misorientation evolution, but this is a challenge for heavily deformed, ultrafine-grained Mg alloys. Grain boundary sliding may also play a major role in the deformation as the grain size decreases to nanoscale.

In summary, a high-strength/high-ductility AZ31 alloy was obtained utilizing a multiple-temperature step-down ECAP approach. The yield strength achieved is the highest reported for AZ31 Mg alloy so far with substantial tensile ductility. There is an apparent change in the H-P behavior of prismatic slip at grain sizes below 1 μm. This change is likely to be due to the earlier activation of basal slip or pyramidal slip, delay in prismatic slip activity due to the basal pole spread, grain boundary sliding, and notable difference in the grain size sensitivity of prismatic and basal slips. It can be concluded that careful control of texture and grain refinement down to submicron levels is possible through multiple-temperature step-down ECAP in truly bulk Mg alloys, which results in unidirectional ultra-high specific strength levels with significant ductility.

This work was funded by the US Army Research Lab through contract W911NF-11-2-0035.

[1] B.L. Mordike, T. Ebert, Mater. Sci. Eng. A 302 (2001) 37.
[2] A. Yamashita, Z. Horita, T.G. Langdon, Mater. Sci. Eng. A 300 (2001) 142.
[3] T. Mukai, M. Yamanoi, H. Watanabe, K. Higashi, Scripta Mater. 45 (2001) 89.
[4] S.R. Agnew, P. Mehrotra, T.M. Lillo, G.M. Stoica, P.K. Liaw, Acta Mater. 53 (2005) 3135.
[5] S.X. Ding, W.T. Lee, C.P. Chang, L.W. Chang, P.W. Kao, Scripta Mater. 59 (2008) 1006.
[6] S. Biswas, S.S. Dhinwal, S. Suwas, Acta Mater. 58 (2010) 3247.
[7] M. Al-Maharbi, I. Karaman, I.J. Beyerlein, D.C. Foley, K.T. Hartwig, L. Kecskes, S. Mathaudhu, Mater. Sci. Eng. A 528 (2011) 7616.
[8] D.C. Foley, M. Al-Maharbi, K.T. Hartwig, I. Karaman, L.J. Kecskes, S.N. Mathaudhu, Scripta Mater. 64 (2011) 193.
[9] R.E. Reedhill, W.D. Robertson, Acta Metall. 5 (1957) 728.
[10] J. Koike, T. Kobayashi, T. Mukai, H. Watanabe, M. Suzuki, K. Maruyama, K. Higashi, Acta Mater. 51 (2003) 2055.
[11] J.A. del Valle, F. Carreno, O.A. Ruano, Acta Mater. 54 (2006) 4247.
[12] A. Jain, O. Duygulu, D.W. Brown, C.N. Tome, S.R. Agnew, Mater. Sci. Eng. A 486 (2008) 545.
[13] Z. Keshavarz, M.R. Barnett, Scripta Mater. 55 (2006) 915.
[14] W. Yuan, S.K. Panigrahi, J.Q. Su, R.S. Mishra, Scripta Mater. 65 (2011) 994.
[15] S.M. Razavi, M.S. Thesis, Texas A&M University, 2011.
[16] M.R. Barnett, Mater. Sci. Eng. A 464 (2007) 8.
[17] I. Ulacia, N.V. Dudamell, F. Galvez, S. Yi, M.T. Perez-Prado, I. Hurtado, Acta Mater. 58 (2010) 2988.
[18] M.R. Barnett, Z. Keshavarz, X. Ma, Metall. Mater. Trans. A 37A (2006) 2283.
[19] S.R. Agnew, C.N. Tome, D.W. Brown, T.M. Holden, S.C. Vogel, Scripta Mater. 48 (2003) 1003.
[20] G. Bhargava, W. Yuan, S.S. Webb, R.S. Mishra, Metall. Mater. Trans. A 41A (2010) 13.
[21] W. Yuan, R.S. Mishra, B. Carlson, R.K. Mishra, R. Verma, R. Kubic, Scripta Mater. 64 (2011) 580.